

Crystal structure and Hirshfeld surface analysis of (*E*)-2-[(anthracen-9-ylmethylidene)amino]-4-nitroaniline

Soukaina Benkirane,^{a*} Houria Misbahi,^a Joel T. Mague,^b Tuncer Hökelek,^c Mazzah Ahmed^d and Nada Kheira Sebbar^e

Received 16 October 2025

Accepted 30 January 2026

Edited by D. R. Manke, University of Massachusetts Dartmouth, USA

Keywords: crystal structure; π -stacking; C—H $\cdots\pi$ (ring) interaction.

CCDC reference: 2527280

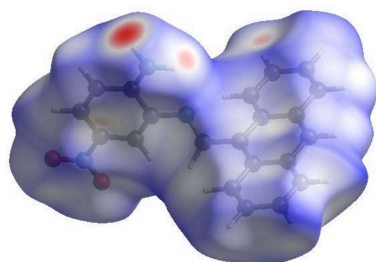
Supporting information: this article has supporting information at journals.iucr.org/e

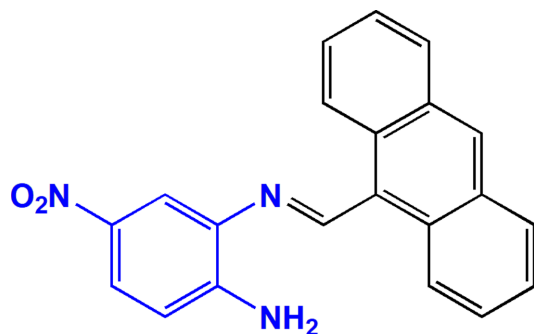
^aLaboratory of Applied Organic Chemistry, Sidi Mohamed Ben Abdellah University, Faculty Of Science And Technology, Road Immouzer, BP 2202 Fez, Morocco, ^bDepartment of Chemistry, Tulane University, New Orleans, LA 70118, USA, ^cDepartment of Physics, Hacettepe University, 06800 Beytepe, Ankara, Türkiye, ^dUniversity of Lille, CNRS, UAR 3290, MSAP, Miniaturization for Synthesis, Analysis and Proteomics, 59000 Lille, France, and ^eLaboratory of Heterocyclic Organic Chemistry, Pharmacochemistry Competence Center, Av. Ibn Battouta, BP 1014, Faculty of Sciences, Mohammed V University, in Rabat, Morocco. *Correspondence e-mail: soukaina.benkirane@usmba.ac.ma

The title compound, C₂₁H₁₅N₃O₂, contains a nitroaniline ring and an anthracene ring system bridged over the methylene amino group. The anthracene ring system is essentially planar with an r.m.s. deviation of 0.03 (2) Å and it is oriented at a dihedral angle of 79.70 (5)° with respect to nitroaniline ring. There is an intramolecular N—H \cdots N hydrogen bond between N atoms of nitroaniline ring and amino group. In the crystal, N—H—O hydrogen bonds link the molecules into infinite chains along the *b*-axis direction. π – π stacking interactions between the nitroaniline rings of adjacent molecules with centroid-to-centroid distance of 3.7682 (2) Å and C—H $\cdots\pi$ (ring) interactions may help to consolidate the three-dimensional architecture. A Hirshfeld surface analysis indicates that the most important contributions for the crystal packing are from H \cdots H (35.5%), H \cdots C/C \cdots H (33.7%) and H \cdots O/O \cdots H (18.3%) interactions.

1. Chemical context

The Schiff base family is a class of organic compounds characterized by the presence of an imine group (Moss *et al.*, 1995; Schiff, 1864). Their structural features confer notable reactivity and versatility, making them valuable scaffolds with numerous applications, such as fluorescent chemosensors (Udhayakumari *et al.*, 2020), as catalysts (Boghaei *et al.*, 2002), in water treatment (Khan *et al.*, 2019) and as corrosion inhibitors (Ashassi-Sorkhabi *et al.*, 2005; Verma & Quraishi, 2021). In medicinal chemistry, numerous investigations have also highlighted their broad spectrum of activities (Hameed *et al.*, 2017; Mushtaq *et al.*, 2024; Nidhi *et al.*, 2025; Younus *et al.*, 2023), notably as anti-microbial (Barakat *et al.*, 2025), anti-cancer (Uddin *et al.*, 2020), anti-inflammatory (Murtaza *et al.*, 2017), antiviral (Azzouzi *et al.*, 2024), anti-diabetic (Adalat *et al.*, 2022), and antioxidant (Madi *et al.*, 2021) agents. Particular focus on derivatives incorporating nitrobenzene or anthracene moieties has demonstrated significant activities (Aravindan *et al.*, 2021; Bai *et al.*, 2017; Gümüş *et al.*, 2020; Kraicheva *et al.*, 2012; Mahmoud *et al.*, 2018). Prompted by these findings, the title compound was synthesized by the condensation of anthracene-9-carbaldehyde and 4-nitrobenzene-1,2-diamine, giving a new Schiff compound containing both anthracene and nitrobenzene moieties. Its synthesis and molecular and crystal structures are described here, along with the results of a Hirshfeld surface analysis.





2. Structural commentary

The title compound, (I), contains an nitroaniline ring (*A*, C1–C6) and an anthracene ring system (*B*, C8–C21) bridged over the methylene amino group (Fig. 1). The anthracene ring system, consisting of three fused benzene rings, is essentially planar with r.m.s. deviation of 0.03 (2) Å and it is oriented at a dihedral angle of 79.70 (5)° with respect to nitroaniline ring *A*. Atoms N1, N2, N3, O1A and O1B are 0.0345 (18), 0.0135 (20), 0.0168 (16), 0.1040 (17) and –0.0276 (18) Å, respectively, away from the best least-squares plane through ring *A*. Thus, they are nearly coplanar. There is an intramolecular N–H···N hydrogen bond (Table 1) between the N atoms of ring *A* and the amino group. No unusual bond lengths or interbond angles are observed.

3. Supramolecular features

In the crystal, N–H···O hydrogen bonds (Table 1) link the molecules into infinite chains along the *b*-axis direction (Fig. 2). π – π stacking interactions between the *A* rings [centroid-to-centroid distance = 3.7682 (2) Å, α = 0.02 (10)° and slippage = 1.375 Å] of adjacent molecules and C–H··· π (ring) interactions (Table 1) may help to consolidate the three-dimensional architecture.

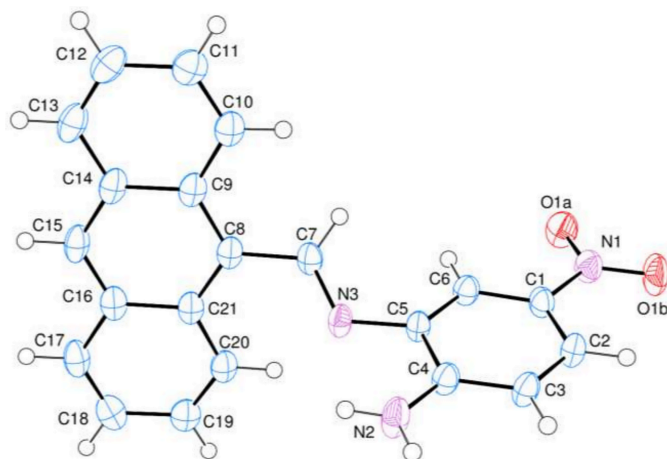


Figure 1
The molecular structure of the title compound (I) showing 50% probability ellipsoids.

Table 1
Hydrogen-bond geometry (Å, °).

Cg1 is the centroid of the C1–C6 ring.

<i>D</i> –H··· <i>A</i>	<i>D</i> –H	H··· <i>A</i>	<i>D</i> ··· <i>A</i>	<i>D</i> –H··· <i>A</i>
N2–H2A···O1B ⁱ	0.88	2.07	2.939 (2)	168
N2–H2B···N3	0.88	2.31	2.672 (2)	104
C19–H19···Cg1 ⁱⁱ	0.95	2.65	3.492 (2)	149

Symmetry codes: (i) $-x, y + \frac{1}{2}, -z + \frac{3}{2}$; (ii) $x, y, z + 1$.

Table 2
Selected interatomic distances (Å).

N2···O1B ⁱ	2.939 (2)	C6···H7	2.71
O1A···H6	2.44	C7···H20	2.66
O1B···H2	2.41	C7···H6	2.81
H2A···O1B ⁱ	2.07	C7···H10	2.58
N2···N3	2.672 (2)	C10···H7	2.75
N3···C20	2.913 (3)	H6···H7	2.39
N3···H2B	2.31	H7···H10	2.19
N3···H20	2.35		

Symmetry code: (i) $-x, y + \frac{1}{2}, -z + \frac{3}{2}$.

4. Hirshfeld surface analysis

A Hirshfeld surface (HS) analysis was carried out using *Crystal Explorer 17.5* (Spackman *et al.*, 2021) to visualize the intermolecular interactions in the crystal. Fig. 3 shows the contact distances where the bright-red spots correspond to the respective donors and/or acceptors. The white surfaces and the red and blue areas indicate contacts with distances equal, shorter and longer, respectively, than the van der Waals radii (Table 2). The π – π stacking and C–H··· π (ring) interactions

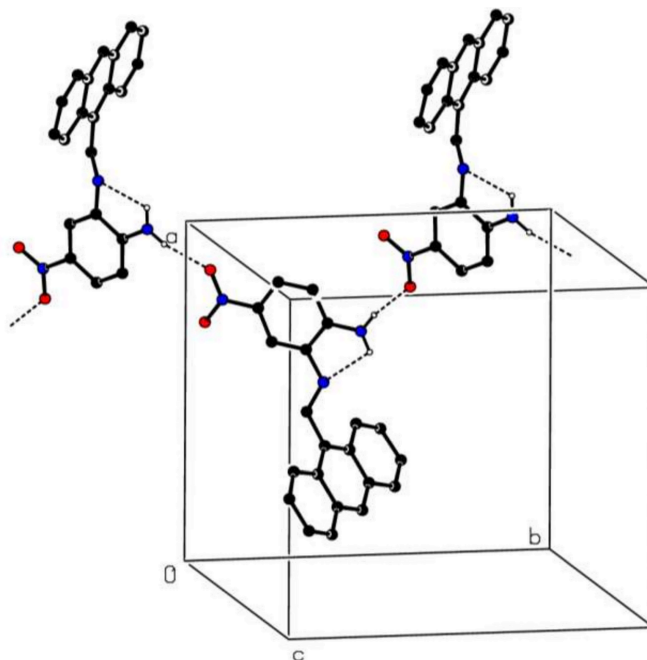


Figure 2
A partial packing diagram of the title compound (I). The intramolecular N–H···N and intermolecular N–H···O hydrogen bonds are shown as dashed lines. Hydrogen atoms not involved in these interactions have been omitted for clarity.

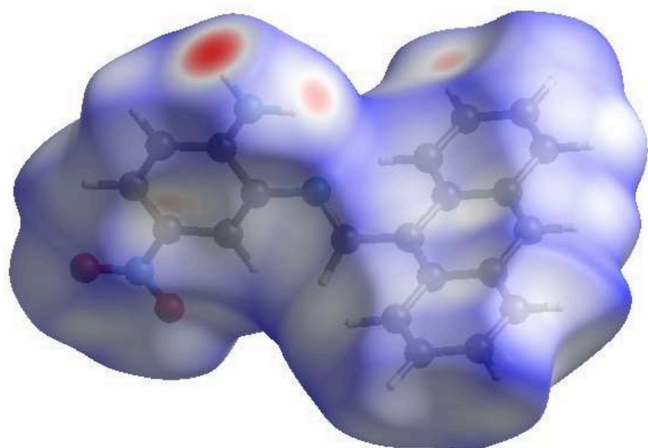


Figure 3
View of the three-dimensional Hirshfeld surface of the title compound (I) plotted over d_{norm} .

are shown in Fig. 4*a* and 4*b* by the presence of the adjacent red and blue triangles and the red π -holes, respectively. According to the two-dimensional fingerprint plots (McKinnon *et al.*, 2007), the $\text{H}\cdots\text{H}$, $\text{H}\cdots\text{C}/\text{C}\cdots\text{H}$ and $\text{H}\cdots\text{O}/\text{O}\cdots\text{H}$ contacts make the most significant contributions to the HS, at 35.5%, 33.7% and 18.3%, respectively (Table 2 and Fig. 5).

5. Database survey

A search of the Cambridge Structural Database (CSD, updated September 2025; Groom *et al.*, 2016) identified seven compounds with structural similarity to the target compound (*E*)-2-[(anthracen-9-ylmethylene)amino]-4-nitroaniline. Structures **I** to **VI** (CSD codes: RIRMAH01, LIJQII, WEFBAM, WAZWAX, WAZVUQ and WAZVOK; Geiger & Parsons, 2014; Goettler & Hamaker, 2022; Dalapati *et al.*, 2012*a,b*) all possess a nitrobenzene ring but do not correspond to Schiff bases. They are distinguished by the nature of their substituents (methyl, phenyl or imidazo[1,2-*a*]pyridin-2-ylmethyl groups) and the possible presence of solvation molecules or anions (H_2O , H_2PO_4^- , HSO_4^- , tetra-*n*-butylammonium). These differences reflect the structural flexibility and the various supramolecular organizations that the nitrobenzene skeleton can adopt. On the other hand, compound **VII** [CSD refcode: SUYSAH, N^2 -(4-chlorobenzylidene)-4-

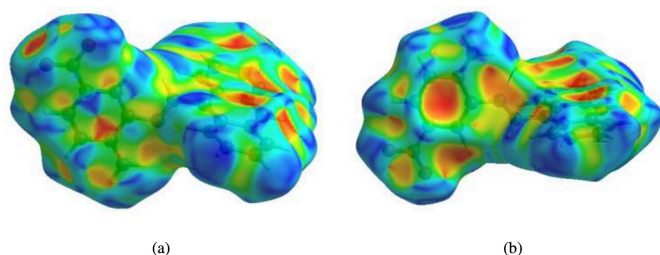


Figure 4
The shape-index surface showing two orientations for (a) π - π stacking and (b) $\text{C}-\text{H}\cdots\pi(\text{ring})$ interactions.

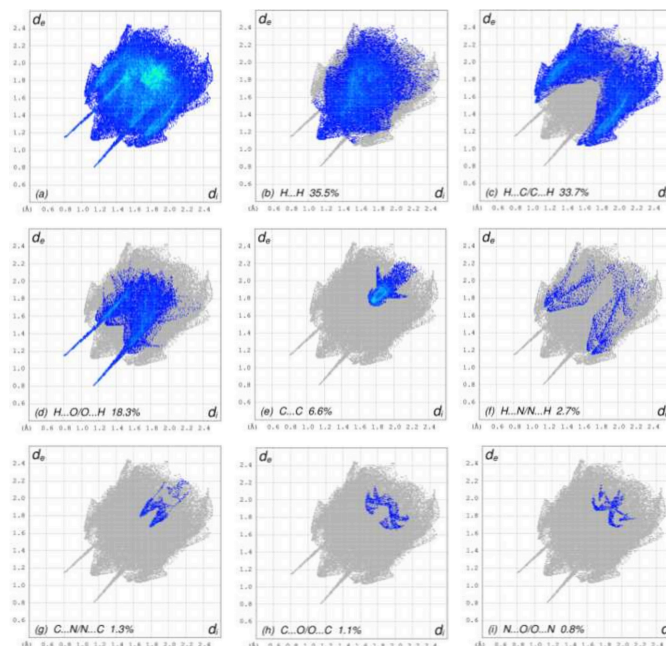
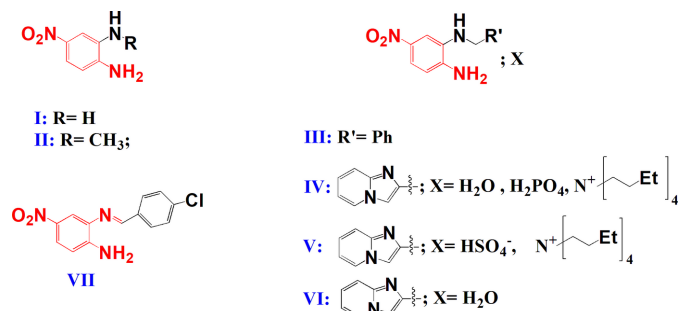


Figure 5
The two-dimensional fingerprint plots of the title compound (I), showing (a) all interactions, and delineated into (b) $\text{H}\cdots\text{H}$, (c) $\text{H}\cdots\text{C}/\text{C}\cdots\text{H}$, (d) $\text{H}\cdots\text{O}/\text{O}\cdots\text{H}$, (e) $\text{C}\cdots\text{C}$, (f) $\text{H}\cdots\text{N}/\text{N}\cdots\text{H}$, (g) $\text{C}\cdots\text{N}/\text{N}\cdots\text{C}$, (h) $\text{C}\cdots\text{O}/\text{O}\cdots\text{C}$ and (i) $\text{N}\cdots\text{O}/\text{O}\cdots\text{N}$ interactions. The d_i and d_e values are the closest internal and external distances (in Å) from given points on the Hirshfeld surface.

nitrobenzene-1,2-diamine; Farag *et al.*, 2010] turns out to be the closest structural analogue of the studied compound and shares the same basic Schiff molecular framework formed by the condensation of a 1,2-diamine derivative and an aromatic aldehyde, as well as a similar electronic arrangement around the azomethine group ($-\text{CH}=\text{N}-$). This analysis highlights the structural consistency of the target compound with the analogues listed in the CSD, while highlighting its originality linked to the presence of the anthracene fragment, likely to influence its electronic and π - π stacking properties in the solid state.



6. Synthesis and crystallization

In a flask, 0.4 g (2.61 mmol) of 4-nitrobenzene-1,2-diamine was stirred into 20 mL of methanol at 323 K until it was completely dissolved. Then, 0.53 g (2.61 mmol) of anthracene-9-carbaldehyde was added in small portions, with the mixture

Table 3
Experimental details.

Crystal data	
Chemical formula	C ₂₁ H ₁₅ N ₃ O ₂
<i>M_r</i>	341.36
Crystal system, space group	Monoclinic, <i>P</i> 2 ₁ / <i>c</i>
Temperature (K)	120
<i>a</i> , <i>b</i> , <i>c</i> (Å)	12.8213 (9), 15.7634 (9), 8.3763 (5)
β (°)	107.140 (7)
<i>V</i> (Å ³)	1617.72 (18)
<i>Z</i>	4
Radiation type	Cu Kα
μ (mm ⁻¹)	0.75
Crystal size (mm)	0.1 × 0.05 × 0.03
Data collection	
Diffractometer	XtaLAB Synergy R, DW system, HyPix
Absorption correction	Multi-scan (<i>CrysAlis PRO</i> ; Rigaku OD, 2022)
<i>T_{min}</i> , <i>T_{max}</i>	0.419, 1.000
No. of measured, independent and observed [<i>I</i> > 2σ(<i>I</i>)] reflections	38890, 2880, 2609
<i>R_{int}</i>	0.094
(sin θ/λ) _{max} (Å ⁻¹)	0.598
Refinement	
<i>R</i> [<i>F</i> ² > 2σ(<i>F</i> ²)], <i>wR</i> (<i>F</i> ²), <i>S</i>	0.053, 0.140, 1.07
No. of reflections	2880
No. of parameters	235
H-atom treatment	H-atom parameters constrained
Δρ _{max} , Δρ _{min} (e Å ⁻³)	0.25, -0.28

Computer programs: *CrysAlis PRO* (Rigaku OD, 2022), *SHELXT2018/2* (Sheldrick, 2015a), *SHELXL2018/3* (Sheldrick, 2015b) and *OLEX2* (Dolomanov *et al.*, 2009).

being warmed to reflux. An orange precipitate formed after 1 h, and the reaction was monitored by TLC until the starting materials were consumed entirely (3 h). The mixture was then cooled to ambient temperature, and the precipitate was collected by filtration. It was washed three times (10 mL) with methanol and dried at 323 K to yield a pure powder. The product was characterized by ¹H and ¹³C NMR, IR and UV-Vis spectroscopy. The slow evaporation of a 2:1 (v/v) mixture of ethyl acetate and methanol was used to obtain single crystals. C₂₁H₁₅N₃O₂; **Colour:** Orange; **Yield:** 98.5%, **R_f** = 0.72 (ethyl acetate/hexane: 1/1), **Melting Point:** 512.9 K; **¹H NMR** (DMSO-*d*₆, 300 MHz): δ (ppm) 6.62 (*s*, 2H, NH₂), 9.95 (*s*, 1H, -CH=N-), 8.81 (*m*, 3H, H_{Ar}), 8.19 (*m*, 3H, H_{Ar}), 8.02 (*d*, 1H, ³J_{H-H} = 9 Hz, H_{Ar}), 7.62 (*m*, 4H, H_{Ar}), 6.89 (*d*, 1H, ³J_{H-H} = 9 Hz, H_{Ar}); **¹³C NMR** (DMSO-*d*₆, 75 MHz): δ (ppm) 127.62, 130.77, 131.30, 136.72, 151.16 (C_q), 160.35 (-CH=N-), 113.29, 114.20, 124.93, 125.53, 126.1, 127.97, 129.40, 131.33 (C_{Ar}); **FT-IR** (cm⁻¹): 3450, 3400 (N-H stretching, -NH₂), 3100, 3000 (aromatic C-H stretching), 1650 (C=N stretching, imine), 1500 (C=C stretching, aromatic ring); **UV-Vis** (DMSO), λ_{max} (nm): 310, 430, 480.

7. Refinement

Crystal data, data collection and structure refinement details are summarized in Table 3. The hydrogen-atom positions were calculated geometrically at N-H = 0.88 Å and C-H = 0.95 Å and refined using a riding model with *U*_{iso}(H) = 1.2 × *U*_{eq}(N, C).

Acknowledgements

TH is grateful to Hacettepe University Scientific Research Project Unit (grant No. 013 D04 602 004). We extend our gratitude to Dr Samia Benmansour, Assistant Professor in the Department of Inorganic Chemistry, University of Valencia (Dr Moliner 50, Burjassot, Valencia, Spain), for her valuable collaboration in the crystallographic analyses.

References

- Adalat, B., Rahim, F., Taha, M., Hayat, S., Iqbal, N., Ali, Z., Shah, S. A. A., Wadood, A., Rehman, A. U. & Khan, K. M. (2022). *J. Mol. Struct.* **1265**, 133287.
- Aravindan, P., Sivaraj, K., Kamal, C., Vennila, P. & Venkatesh, G. (2021). *J. Mol. Struct.* **1229**, 129488.
- Ashassi-Sorkhabi, H., Shaabani, B. & Seifzadeh, D. (2005). *Appl. Surf. Sci.* **239**, 154–164.
- Azzouzi, M., Ouchouai, A. A., Azougagh, O., El Hadad, S. E., Abou-salama, M., Oussaid, A., Pannecouque, C. & Rohand, T. (2024). *RSC Adv.* **14**, 36902–36918.
- Bai, J., Wang, R. H., Qiao, Y., Wang, A. & Fang, C. J. (2017). *Drug. Des. Dev. Ther.* **11**, 2227–2237.
- Barakat, A., Ehagali, G. A. M., Kamoun, E. A., Abusaif, M. S., Owda, M. E., Ghazy, M. B. & Ammar, Y. A. (2025). *Carbohydr. Polym.* **352**, 123205.
- Boghaei, D. M. & Mohebi, S. (2002). *J. Mol. Catal. A Chem.* **179**, 41–51.
- Dalapati, S., Alam, M. A., Jana, S. & Guchhait, N. (2012a). *Crys-tEngComm* **14**, 6029–6034.
- Dalapati, S., Alam, M. A., JANA, S., Saha, R., Biswas, S. & Guchhait, N. (2012b). *ChemPlusChem* **77**, 93–97.
- Dolomanov, O. V., Bourhis, L. J., Gildea, R. J., Howard, J. A. K. & Puschmann, H. (2009). *J. Appl. Cryst.* **42**, 339–341.
- Farag, A. M., Guan, T. S., Osman, H., Rosli, M. M. & Fun, H.-K. (2010). *Acta Cryst.* **E66**, o2220.
- Geiger, D. K. & Parsons, D. E. (2014). *Acta Cryst.* **C70**, 681–688.
- Goettler, P. E. & Hamaker, C. G. (2022). *J. Chem. Crystallogr.* **52**, 251–259.
- Groom, C. R., Bruno, I. J., Lightfoot, M. P. & Ward, S. C. (2016). *Acta Cryst.* **B72**, 171–179.
- Gümüş, A., Okumuş, V. & Gümüüş, S. (2020). *Turk. J. Chem.* **44**, 1200–1215.
- Hameed, A., al-Rashida, M., Uroos, M., Abid Ali, S. & Khan, K. M. (2017). *Expert Opin. Ther. Pat.* **27**, 63–79.
- Khan, S., Qureshi, I., Shifa, M. S. & Waziri, A. H. (2019). *Int. J. Environ. Anal. Chem.* **99**, 1123–1134.
- Kraicheva, I., Tsacheva, I., Vodenicharova, E., Tashev, E., Tosheva, T., Kril, A., Topashka-Ancheva, M., Iliev, I., Gerasimova, T. & Troev, K. (2012). *Bioorg. Med. Chem.* **20**, 117–124.
- Madi, A. A., Haffar, D., Benganem, F., Ghedjati, S., Toukal, L., Dorcet, V. & Bourzami, R. (2021). *J. Mol. Struct.* **1227**, 129368.
- Mahmoud, W. H., Deghadi, R. G. & Mohamed, G. G. (2018). *Appl. Organomet. Chem.* **32**, e4289.
- McKinnon, J. J., Jayatilaka, D. & Spackman, M. A. (2007). *Chem. Commun.* 3814–3816.
- Moss, G. P., Smith, P. A. S. & Tavernier, D. (1995). *Pure Appl. Chem.* **67**, 1307–1375.
- Murtaza, S., Akhtar, M. S., Kanwal, F., Abbas, A., Ashiq, S. & Shamim, S. (2017). *J. Saudi Chem. Soc.* **21**, S359–S372.
- Mushtaq, I., Ahmad, M., Saleem, M. & Ahmed, A. (2024). *Futur J. Pharm. Sci.* **10**, 16.
- Nidhi, Siddharam, Rao, D. P., Gautam, A. K., Verma, A. & Gautam, Y. (2025). *Results Chem.* **13**, 101941.

- Rigaku OD (2022). *CrysAlis PRO*. Rigaku Oxford Diffraction, Yarnton, England.
- Schiff, H. (1864). *Justus Liebigs Ann. Chem.* **131**, 118–119.
- Sheldrick, G. M. (2015a). *Acta Cryst.* **A71**, 3–8.
- Sheldrick, G. M. (2015b). *Acta Cryst.* **C71**, 3–8.
- Spackman, P. R., Turner, M. J., McKinnon, J. J., Wolff, S. K., Grimwood, D. J., Jayatilaka, D. & Spackman, M. A. (2021). *J. Appl. Cryst.* **54**, 1006–1011.
- Uddin, N., Rashid, F., Ali, S., Tirmizi, S. A., Ahmad, I., Zaib, S., Zubair, M., Diaconescu, P. L., Tahir, M. N., Iqbal, J. & Haider, A. (2020). *J. Biomol. Struct. Dyn.* **38**, 3246–3259.
- Udhayakumari, D. & Inbaraj, V. (2020). *J. Fluoresc.* **30**, 1203–1223.
- Verma, C. & Quraishi, M. A. (2021). *Coord. Chem. Rev.* **446**, 214105.
- Younus, H. A., Saleem, F., Hameed, A., Al-Rashida, M., Al-Qawasmeh, R. A., El-Naggar, M., Rana, S., Saeed, M. & Khan, K. M. (2023). *Expert Opin. Ther. Pat.* **33**, 841–864.

supporting information

Acta Cryst. (2026). E82, 259-263 [https://doi.org/10.1107/S2056989026001027]

Crystal structure and Hirshfeld surface analysis of (*E*)-2-[(anthracen-9-ylmethylidene)amino]-4-nitroaniline

Soukaina Benkirane, Houria Misbahi, Joel T. Mague, Tuncer Hökelek, Mazzah Ahmed and Nada Kheira Sebbar

Computing details

(*E*)-2-[(Anthracen-9-ylmethylidene)amino]-4-nitroaniline

Crystal data

$C_{21}H_{15}N_3O_2$

$M_r = 341.36$

Monoclinic, $P2_1/c$

$a = 12.8213$ (9) Å

$b = 15.7634$ (9) Å

$c = 8.3763$ (5) Å

$\beta = 107.140$ (7)°

$V = 1617.72$ (18) Å³

$Z = 4$

$F(000) = 712$

$D_x = 1.402$ Mg m⁻³

Cu $K\alpha$ radiation, $\lambda = 1.54184$ Å

Cell parameters from 19910 reflections

$\theta = 3.6$ – 66.6 °

$\mu = 0.75$ mm⁻¹

$T = 120$ K

Prism, orange

$0.1 \times 0.05 \times 0.03$ mm

Data collection

XtaLAB Synergy R, DW system, HyPix diffractometer

Radiation source: Rotating-anode X-ray tube, Rigaku (Cu) X-ray Source

Mirror monochromator

Detector resolution: 10.0000 pixels mm⁻¹

ω scans

Absorption correction: multi-scan (CrysAlisPro; Rigaku OD, 2022)

$T_{\min} = 0.419$, $T_{\max} = 1.000$

38890 measured reflections

2880 independent reflections

2609 reflections with $I > 2\sigma(I)$

$R_{\text{int}} = 0.094$

$\theta_{\max} = 67.1$ °, $\theta_{\min} = 3.6$ °

$h = -15 \rightarrow 15$

$k = -18 \rightarrow 18$

$l = -9 \rightarrow 9$

Refinement

Refinement on F^2

Least-squares matrix: full

$R[F^2 > 2\sigma(F^2)] = 0.053$

$wR(F^2) = 0.140$

$S = 1.07$

2880 reflections

235 parameters

0 restraints

Primary atom site location: dual

Hydrogen site location: inferred from neighbouring sites

H-atom parameters constrained

$w = 1/[\sigma^2(F_o^2) + (0.0631P)^2 + 1.1761P]$

where $P = (F_o^2 + 2F_c^2)/3$

$(\Delta/\sigma)_{\max} < 0.001$

$\Delta\rho_{\max} = 0.25$ e Å⁻³

$\Delta\rho_{\min} = -0.28$ e Å⁻³

Special details

Geometry. All esds (except the esd in the dihedral angle between two l.s. planes) are estimated using the full covariance matrix. The cell esds are taken into account individually in the estimation of esds in distances, angles and torsion angles; correlations between esds in cell parameters are only used when they are defined by crystal symmetry. An approximate (isotropic) treatment of cell esds is used for estimating esds involving l.s. planes.

Fractional atomic coordinates and isotropic or equivalent isotropic displacement parameters (\AA^2)

	<i>x</i>	<i>y</i>	<i>z</i>	$U_{\text{iso}}^*/U_{\text{eq}}$
O1A	0.11419 (12)	0.33297 (9)	0.7317 (2)	0.0445 (4)
O1B	−0.01412 (13)	0.37615 (10)	0.8334 (2)	0.0488 (4)
N3	0.25699 (13)	0.60375 (9)	0.5409 (2)	0.0288 (4)
N1	0.05785 (14)	0.39013 (11)	0.7645 (2)	0.0360 (4)
N2	0.12391 (14)	0.72245 (11)	0.5991 (3)	0.0419 (5)
H2A	0.082433	0.763631	0.617169	0.050*
H2B	0.176255	0.733782	0.554024	0.050*
C5	0.17698 (14)	0.57686 (12)	0.6150 (2)	0.0264 (4)
C21	0.40967 (15)	0.61781 (11)	0.3369 (3)	0.0285 (4)
C8	0.43686 (15)	0.59916 (11)	0.5097 (2)	0.0277 (4)
C16	0.49189 (16)	0.65214 (11)	0.2696 (3)	0.0308 (4)
C7	0.35290 (15)	0.57129 (11)	0.5861 (2)	0.0280 (4)
H7	0.370033	0.528682	0.670048	0.034*
C4	0.10739 (15)	0.64265 (12)	0.6402 (2)	0.0300 (4)
C6	0.16031 (15)	0.49425 (12)	0.6552 (2)	0.0286 (4)
H6	0.205506	0.449991	0.636113	0.034*
C14	0.62579 (15)	0.64459 (12)	0.5440 (3)	0.0316 (4)
C15	0.59693 (16)	0.66442 (12)	0.3750 (3)	0.0333 (5)
H15	0.650864	0.687170	0.330052	0.040*
C3	0.02430 (16)	0.62217 (12)	0.7127 (3)	0.0318 (4)
H3	−0.021416	0.665753	0.732859	0.038*
C20	0.30485 (16)	0.60228 (12)	0.2218 (3)	0.0319 (4)
H20	0.249363	0.577762	0.261119	0.038*
C10	0.57722 (16)	0.59476 (12)	0.7901 (3)	0.0327 (4)
H10	0.525540	0.572088	0.839747	0.039*
C1	0.07603 (15)	0.47650 (12)	0.7242 (2)	0.0294 (4)
C9	0.54482 (15)	0.61075 (11)	0.6148 (3)	0.0295 (4)
C17	0.46355 (18)	0.67369 (12)	0.0969 (3)	0.0361 (5)
H17	0.517281	0.698110	0.053462	0.043*
C2	0.00881 (16)	0.53992 (13)	0.7543 (3)	0.0316 (4)
H2	−0.047228	0.526443	0.803246	0.038*
C19	0.28237 (17)	0.62179 (12)	0.0565 (3)	0.0345 (5)
H19	0.212222	0.609453	−0.017515	0.041*
C13	0.73284 (16)	0.66070 (13)	0.6513 (3)	0.0378 (5)
H13	0.786633	0.682713	0.605152	0.045*
C18	0.36215 (18)	0.66023 (13)	−0.0065 (3)	0.0372 (5)
H18	0.344359	0.676395	−0.120670	0.045*
C11	0.68046 (17)	0.61122 (13)	0.8878 (3)	0.0377 (5)
H11	0.699748	0.599779	1.004218	0.045*

C12	0.75971 (17)	0.64530 (14)	0.8178 (3)	0.0402 (5)
H12	0.831298	0.657280	0.887402	0.048*

Atomic displacement parameters (Å²)

	U^{11}	U^{22}	U^{33}	U^{12}	U^{13}	U^{23}
O1A	0.0455 (9)	0.0245 (7)	0.0688 (11)	0.0010 (6)	0.0252 (8)	0.0059 (7)
O1B	0.0479 (9)	0.0385 (9)	0.0720 (11)	-0.0101 (7)	0.0364 (9)	0.0093 (8)
N3	0.0309 (8)	0.0226 (8)	0.0399 (9)	-0.0006 (6)	0.0214 (7)	-0.0013 (6)
N1	0.0343 (9)	0.0299 (9)	0.0462 (10)	-0.0051 (7)	0.0158 (8)	0.0043 (7)
N2	0.0407 (10)	0.0231 (9)	0.0747 (13)	0.0032 (7)	0.0369 (10)	0.0030 (8)
C5	0.0263 (9)	0.0250 (9)	0.0321 (10)	-0.0018 (7)	0.0150 (8)	-0.0003 (7)
C21	0.0336 (10)	0.0163 (8)	0.0427 (11)	0.0027 (7)	0.0223 (9)	-0.0031 (7)
C8	0.0306 (10)	0.0161 (8)	0.0426 (11)	0.0027 (7)	0.0206 (8)	-0.0024 (7)
C16	0.0375 (10)	0.0189 (9)	0.0441 (11)	0.0016 (7)	0.0244 (9)	-0.0042 (8)
C7	0.0325 (10)	0.0183 (8)	0.0381 (11)	-0.0009 (7)	0.0182 (8)	-0.0008 (7)
C4	0.0291 (10)	0.0245 (9)	0.0403 (11)	-0.0003 (7)	0.0165 (8)	-0.0010 (8)
C6	0.0284 (9)	0.0256 (10)	0.0348 (10)	-0.0002 (7)	0.0139 (8)	-0.0013 (8)
C14	0.0302 (10)	0.0225 (9)	0.0493 (12)	0.0022 (7)	0.0228 (9)	-0.0069 (8)
C15	0.0347 (11)	0.0256 (10)	0.0499 (12)	-0.0015 (8)	0.0285 (9)	-0.0063 (8)
C3	0.0278 (10)	0.0289 (10)	0.0443 (11)	0.0002 (7)	0.0194 (9)	-0.0037 (8)
C20	0.0345 (10)	0.0245 (9)	0.0433 (12)	0.0023 (8)	0.0218 (9)	-0.0025 (8)
C10	0.0336 (10)	0.0251 (10)	0.0446 (12)	0.0034 (8)	0.0197 (9)	-0.0022 (8)
C1	0.0298 (10)	0.0252 (9)	0.0359 (10)	-0.0039 (7)	0.0141 (8)	0.0025 (8)
C9	0.0306 (10)	0.0193 (9)	0.0448 (11)	0.0034 (7)	0.0207 (9)	-0.0045 (8)
C17	0.0460 (12)	0.0259 (10)	0.0467 (12)	-0.0027 (8)	0.0296 (10)	-0.0039 (8)
C2	0.0270 (9)	0.0345 (10)	0.0381 (11)	-0.0045 (8)	0.0167 (8)	-0.0012 (8)
C19	0.0376 (11)	0.0281 (10)	0.0417 (12)	0.0030 (8)	0.0177 (9)	-0.0050 (8)
C13	0.0296 (10)	0.0347 (11)	0.0555 (14)	-0.0008 (8)	0.0227 (10)	-0.0094 (9)
C18	0.0521 (13)	0.0282 (10)	0.0377 (11)	0.0017 (9)	0.0230 (10)	-0.0022 (8)
C11	0.0370 (11)	0.0350 (11)	0.0435 (12)	0.0060 (9)	0.0157 (9)	-0.0034 (9)
C12	0.0286 (10)	0.0395 (12)	0.0537 (14)	0.0009 (9)	0.0141 (9)	-0.0103 (10)

Geometric parameters (Å, °)

O1A—N1	1.235 (2)	C14—C9	1.441 (3)
O1B—N1	1.244 (2)	C14—C13	1.424 (3)
N3—C5	1.412 (2)	C15—H15	0.9500
N3—C7	1.282 (2)	C3—H3	0.9500
N1—C1	1.438 (2)	C3—C2	1.372 (3)
N2—H2A	0.8800	C20—H20	0.9500
N2—H2B	0.8800	C20—C19	1.363 (3)
N2—C4	1.337 (3)	C10—H10	0.9500
C5—C4	1.424 (3)	C10—C9	1.425 (3)
C5—C6	1.377 (3)	C10—C11	1.361 (3)
C21—C8	1.417 (3)	C1—C2	1.391 (3)
C21—C16	1.439 (3)	C17—H17	0.9500
C21—C20	1.425 (3)	C17—C18	1.350 (3)

C8—C7	1.472 (2)	C2—H2	0.9500
C8—C9	1.416 (3)	C19—H19	0.9500
C16—C15	1.389 (3)	C19—C18	1.418 (3)
C16—C17	1.425 (3)	C13—H13	0.9500
C7—H7	0.9500	C13—C12	1.357 (3)
C4—C3	1.410 (3)	C18—H18	0.9500
C6—H6	0.9500	C11—H11	0.9500
C6—C1	1.396 (3)	C11—C12	1.420 (3)
C14—C15	1.389 (3)	C12—H12	0.9500
N2…O1B ⁱ	2.939 (2)	C6…H7	2.71
O1A…H6	2.44	C7…H20	2.66
O1B…H2	2.41	C7…H6	2.81
H2A…O1B ⁱ	2.07	C7…H10	2.58
N2…N3	2.672 (2)	C10…H7	2.75
N3…C20	2.913 (3)	H6…H7	2.39
N3…H2B	2.31	H7…H10	2.19
N3…H20	2.35		
C7—N3—C5	120.54 (16)	C2—C3—C4	120.67 (18)
O1A—N1—O1B	122.45 (17)	C2—C3—H3	119.7
O1A—N1—C1	119.49 (16)	C21—C20—H20	119.2
O1B—N1—C1	118.06 (17)	C19—C20—C21	121.54 (19)
H2A—N2—H2B	120.0	C19—C20—H20	119.2
C4—N2—H2A	120.0	C9—C10—H10	119.2
C4—N2—H2B	120.0	C11—C10—H10	119.2
N3—C5—C4	114.51 (16)	C11—C10—C9	121.50 (19)
C6—C5—N3	125.19 (16)	C6—C1—N1	119.07 (17)
C6—C5—C4	120.23 (16)	C2—C1—N1	119.07 (17)
C8—C21—C16	119.36 (18)	C2—C1—C6	121.86 (17)
C8—C21—C20	123.68 (17)	C8—C9—C14	118.87 (18)
C20—C21—C16	116.93 (18)	C8—C9—C10	123.50 (18)
C21—C8—C7	121.00 (17)	C10—C9—C14	117.55 (18)
C9—C8—C21	120.62 (17)	C16—C17—H17	119.2
C9—C8—C7	118.32 (18)	C18—C17—C16	121.55 (19)
C15—C16—C21	119.19 (19)	C18—C17—H17	119.2
C15—C16—C17	121.46 (18)	C3—C2—C1	119.28 (17)
C17—C16—C21	119.35 (19)	C3—C2—H2	120.4
N3—C7—C8	120.87 (17)	C1—C2—H2	120.4
N3—C7—H7	119.6	C20—C19—H19	119.5
C8—C7—H7	119.6	C20—C19—C18	121.0 (2)
N2—C4—C5	119.56 (17)	C18—C19—H19	119.5
N2—C4—C3	121.54 (17)	C14—C13—H13	119.3
C3—C4—C5	118.87 (17)	C12—C13—C14	121.47 (19)
C5—C6—H6	120.5	C12—C13—H13	119.3
C5—C6—C1	119.04 (17)	C17—C18—C19	119.5 (2)
C1—C6—H6	120.5	C17—C18—H18	120.2
C15—C14—C9	119.64 (18)	C19—C18—H18	120.2

C15—C14—C13	121.36 (18)	C10—C11—H11	119.6
C13—C14—C9	118.94 (19)	C10—C11—C12	120.8 (2)
C16—C15—H15	118.9	C12—C11—H11	119.6
C14—C15—C16	122.27 (18)	C13—C12—C11	119.8 (2)
C14—C15—H15	118.9	C13—C12—H12	120.1
C4—C3—H3	119.7	C11—C12—H12	120.1
O1A—N1—C1—C6	-2.7 (3)	C7—C8—C9—C14	-175.00 (15)
O1A—N1—C1—C2	176.97 (19)	C7—C8—C9—C10	1.7 (3)
O1B—N1—C1—C6	176.55 (18)	C4—C5—C6—C1	-1.5 (3)
O1B—N1—C1—C2	-3.8 (3)	C4—C3—C2—C1	-0.1 (3)
N3—C5—C4—N2	-2.2 (3)	C6—C5—C4—N2	-179.33 (19)
N3—C5—C4—C3	179.62 (17)	C6—C5—C4—C3	2.5 (3)
N3—C5—C6—C1	-178.32 (17)	C6—C1—C2—C3	1.1 (3)
N1—C1—C2—C3	-178.57 (18)	C14—C13—C12—C11	0.9 (3)
N2—C4—C3—C2	-179.8 (2)	C15—C16—C17—C18	178.65 (18)
C5—N3—C7—C8	-179.82 (16)	C15—C14—C9—C8	-0.5 (3)
C5—C4—C3—C2	-1.7 (3)	C15—C14—C9—C10	-177.41 (16)
C5—C6—C1—N1	179.36 (17)	C15—C14—C13—C12	176.69 (18)
C5—C6—C1—C2	-0.3 (3)	C20—C21—C8—C7	-7.4 (3)
C21—C8—C7—N3	-38.6 (3)	C20—C21—C8—C9	175.56 (16)
C21—C8—C9—C14	2.1 (3)	C20—C21—C16—C15	-176.78 (16)
C21—C8—C9—C10	178.78 (16)	C20—C21—C16—C17	4.0 (2)
C21—C16—C15—C14	0.1 (3)	C20—C19—C18—C17	3.5 (3)
C21—C16—C17—C18	-2.1 (3)	C10—C11—C12—C13	-0.8 (3)
C21—C20—C19—C18	-1.5 (3)	C9—C8—C7—N3	138.46 (18)
C8—C21—C16—C15	1.5 (3)	C9—C14—C15—C16	-0.6 (3)
C8—C21—C16—C17	-177.80 (16)	C9—C14—C13—C12	-0.3 (3)
C8—C21—C20—C19	179.61 (17)	C9—C10—C11—C12	0.2 (3)
C16—C21—C8—C7	174.45 (15)	C17—C16—C15—C14	179.34 (17)
C16—C21—C8—C9	-2.6 (3)	C13—C14—C15—C16	-177.57 (17)
C16—C21—C20—C19	-2.2 (3)	C13—C14—C9—C8	176.56 (16)
C16—C17—C18—C19	-1.6 (3)	C13—C14—C9—C10	-0.3 (3)
C7—N3—C5—C4	142.86 (18)	C11—C10—C9—C8	-176.31 (17)
C7—N3—C5—C6	-40.1 (3)	C11—C10—C9—C14	0.4 (3)

Symmetry code: (i) $-x, y+1/2, -z+3/2$.

Hydrogen-bond geometry (\AA , $^\circ$)

Cg1 is the centroid of the C1–C6 ring.

$D-H\cdots A$	$D-H$	$H\cdots A$	$D\cdots A$	$D-H\cdots A$
N2—H2A \cdots O1B ⁱ	0.88	2.07	2.939 (2)	168
N2—H2B \cdots N3	0.88	2.31	2.672 (2)	104
C19—H19 \cdots Cg1 ⁱⁱ	0.95	2.65	3.492 (2)	149

Symmetry codes: (i) $-x, y+1/2, -z+3/2$; (ii) $x, y, z+1$.